Directing Supramolecular Nanoparticle Binding onto Polymer Films: Film Formation and Influence of Receptor Density on Binding Densities

Wolfgang H. Binder,*,† Christian Kluger,† Marina Josipovic,† Christoph J. Straif,‡ and Gernot Friedbacher‡

Institute of Applied Synthetic Chemistry/Division Macromolecular Chemistry, Vienna University of Technology, Getreidemarkt 9/163/MC, A-1060 Wien, Austria, and Institute of Chemical Technologies and Analytics, Vienna University of Technology, Getreidemarkt 9/164 IAC, A-1060 Wien, Austria

Received June 6, 2006; Revised Manuscript Received September 19, 2006

ABSTRACT: We report on the deposition of nanoparticles onto polymeric surfaces by use of a multiple hydrogen bonding interaction. Main interest concerned the preparation of statistical copolymers with a defined number of interactions within the side chain, thus enabling control of the number of supramolecular interactions present on the surface for the subsequent binding-process. Thus, statistical copolymers of poly(oxy)norbornenes bearing either perfluorinated side chains or the "Hamilton receptor" in amounts ranging from 1 to 70 mol % were prepared using a ROMP methodology combined with subsequent azide/alkine "click" reactions. Films cast from these polymers—either via spin- or via dip-coating—were used to study the binding of barbituric acid-functionalized Au nanoparticles (diameter = 5 nm) bearing the matching supramolecular interaction toward the Hamilton receptor on the polymeric surface. A detailed AFM analysis of the films was performed, detailing the influence of film-casting conditions on the properties of the final polymeric films. A strong effect on the bound density of the NP's was observed only at lower concentrations (below 1 mol %) of the supramolecular receptor, whereas higher amounts of receptor units exhibit only minor effects on the density of bound nanoparticles. Thus, the presented method offers the generation of polymeric films with a defined density of nanoparticles bound to their surfaces.

Introduction

The deposition of nanoparticles onto surfaces by self-assembly processes represents an important contribution for exploiting the important physicochemical properties of these materials.[1] A variety of principles have been exploited to effect the spatial organization of nanoparticles (NPs) using methods such as (a) deposition onto self-assembled monolayers,[2] (b) the use of interfacial forces to effect NP aggregation at liquid/liquid and liquid/gas interfaces,[3] and (c) evaporation-controlled deposition and directed supramolecular forces to effect selective binding events between NPs and appropriately functionalized surfaces.[4] Particular interest has been put toward the deposition of NPs onto polymeric surfaces,[1a,5,6] since a variety of important physical properties can be effected with thin polymeric films, whereupon deposited nanoaprticles can form functional layers for electronic, magnetic, and optical applications. Important contributions in this aspect include the use of NP layers for photoinduced electron transport to metal electrodes[7] as well as specific use of sensors upon small ligand binding.[8]

Still, controlling the deposition of nanosized objects onto surfaces is among the important endeavors in interfacial science. As a basic process upon binding of an object onto a surface, the kinetic energy of the nanosized objects is sacrificed, resulting in a significant entropic loss due to immobilization onto the surface. Thus, the alignment of nanoparticles and related, smaller objects sized below 100 nm is more difficult to achieve than with their larger-sized counterpart in the micron-sized regime: as particles grow smaller, their kinetic energy in solution is increased, resulting in a reduced tendency of ordering, as demonstrated at liquid/liquid interfaces: Thus, NPs with sizes below 2.5 nm usually cannot form ordered arrays at the interface, since the thermal energy/particle exceeds the energy gain due to assembly.[1a,9] Thus, higher energy interactions such as directed supramolecular interactions have been investigated to effect a tighter binding of NPs at surfaces. Examples toward this endeavor are (a) hydrogen bonding interaction, (b) hydrophobic interactions, and (c) electrostatic forces. Usually, matching supramolecular interactions are affixed onto the NP's and the interaction surface, where the NP should be bound to. Relevant recent examples comprise cyclodextrin/adamantane interactions,[2,10] thymine/triazine interaction,[8,11] and the Hamilton receptor/barbituric acid interaction.[2b,6a,12] Since some of these interactions are too weak to effect the binding of smaller-sized NPs, multiple copies of weaker interactions are required, according to a concept reviewed by Whitesides et al.[13] Thus, Reinhoudt et al.[2,10] have used molecular printboards in the form of deposited dendrimers to display multiple binding sites of the cyclodextrine/adamantane interaction to promote the deposition of silica NPs (sized ∼20 nm). Only with these multiple-binding concepts was a stable and efficient binding possible. We recently[2b,6a] have reported on the binding of 5 and 20 nm Au NPs onto either self-assembled monolayers or block copolymeric films by use of a multiple hydrogen bonding interaction (Hamilton receptor/barbituric acid interaction). It was demonstrated that dense layers of NPs could be achieved, resulting in spatially resolved patterns due to the high selectivity and specificity of the supramolecular interaction. Most importantly, the use of a block copolymer bearing multiple copies of the Hamilton receptor in one block (namely 50 copies in one block) lead to the formation of island of surface-bound NPs, concentrated in domain sizes corresponding to the initial block structure of the block copolymer.[6a]

† Institute of Applied Synthetic Chemistry/Division Macromolecular Chemistry.
‡ Institute of Chemical Technologies and Analytics.
* Corresponding author. E-mail: wbinder@mail.zserv.tuwien.ac.at.

10.1021/ma061256d CCC: $33.50
Published on Web 10/24/2006

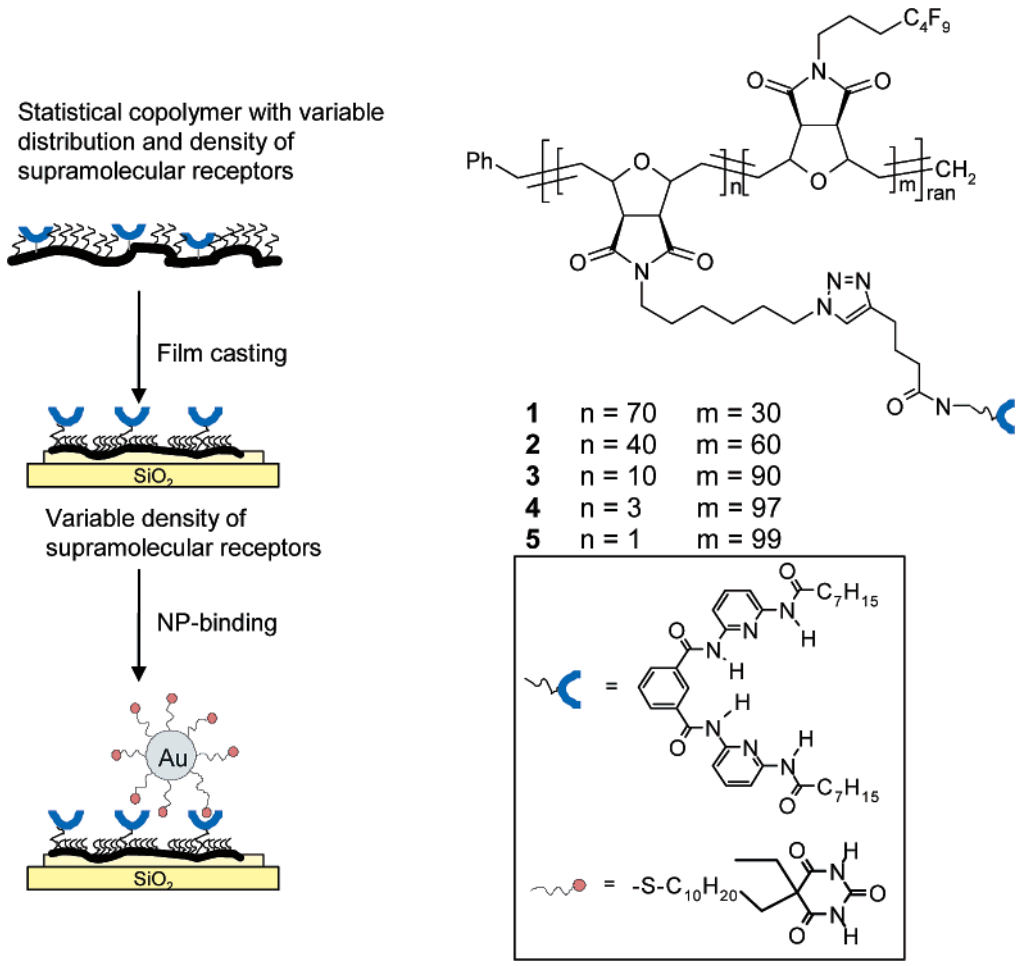

Figure 1. Concept of nanoparticle binding onto a copolymer film prepared from a statistical copolymer bearing a supramolecular receptor ("Hamilton receptor") and an inert, perfluoroalkyl side chain. The statistical copolymer with molecular fractions of the supramolecular receptor ranging from 70 to 1 mol % is cast as a thin film, whereupon nanoparticles (Au NP, diameter = 5 nm) bearing the matching hydrogen bonding receptor are bound by multiple hydrogen bonding interaction ($K_{assn} \sim 10^5$ M^{-1}).

In the present paper we report the binding of NPs onto films consisting of statistical copolymers as depicted in Figure 1. Using this approach, a defined tuning of the receptor density on the polymeric surface can be achieved, leading to polymeric films with a controllable receptor density on the surface. The well-known Hamilton receptor/barbituric acid interaction[12] with a binding constant of $\sim 10^5$ M^{-1} was used, as reported by us[12a-e] previously. Subsequently, these films were used to effect the supramolecular binding of NPs, enabling to study the influence of the receptor density on the polymer film in relation to the number of bound NPs. A critical point concerned the preparation of random copolymers with a defined receptor density within their chain. Therefore, in the following the preparation of such statistical copolymers with a defined density of receptors as well as their film formation and subsequent NP binding are reported.

Experimental Section

General. ^{1}H and ^{13}C spectra were recorded at room temperature on a Bruker AC-E-200 (200 MHz) and a Bruker Avance DRX-400 (400 MHz) FT-NMR spectrometer. $CDCl_3$ (Isotec Inc., 99.8 at. % D) and DMSO-d_6 (HDO + D_2O < 0.02%) were used as solvents. Chemical shifts were recorded in parts per million (δ) and referenced to residual protonated solvent ($CDCl_3$: 7.26 ppm (^{1}H) and 77.0 ppm (^{13}C); DMSO-d_6: 2.54 ppm (^{1}H) and 40.45 ppm (^{13}C)). GPC analysis was performed on a Viscothek VE 2001 system using Styragel linear columns in THF at 40 °C. Polystyrene standards were used for conventional external calibration using a Waters RI 2410 refractive index detector.

AFM Measurements. For the AFM investigations a NanoScope III multimode SPM from Digital Instruments, Veeco Metrology Group, Santa Barbara, CA, has been used. Measurements were performed in tapping mode under ambient air using single-crystal silicon cantilevers (Arrow NC cantilevers, NanoWorld, Switzerland, spring constant 42 N/m, resonance frequency ~285 kHz). Scanning was accomplished with an E-scanner (maximum scan range 10 μm × 10 μm) operated at a scanning rate of 2 Hz and an image resolution of 512 × 512 pixels. Data evaluation was performed with the NanoScope software version 6.13r1 (Digital Instruments, Veeco). The roughness data used in this paper are root-mean-square (rms) values, derived as standard deviations of all height values in an image. Phase images (i.e., the phase lag between the piezo-oscillation driving the AFM cantilever and its response) were recorded simultaneously with the topographic images through the second data channel of the instrument.

Solvents/Reagents. Methanol was dried over CaH_2 refluxing for 24 h, distilled, and stored with activated Klinosorb 3 Å molecular sieve. Tetrahydrofuran (THF) was refluxed over sodium wires and benzophenone overnight, distilled, and stored with activated Klinosorb 4 Å molecular sieve. Chloroform and dichloromethane were refluxed over K_2CO_3, distilled, and stored with activated Klinosorb 4 Å molecular sieve. DMF was refluxed with calcium hydride, distilled, and stored with activated Klinosorb 4 Å molecular sieve. Toluene was refluxed over sodium, distilled, and stored with Klinosorb 4 Å molecular sieve. Triethylamine was purchased from Aldrich and refluxed 2 h over calcium hydride prior to use. Benzylidene−bis(tricyclohexylphosphine)dichlororuthenium (Grubbs first-generation catalyst) (**9**), tetrakis(acetonitrile)hexafluorophosphate copper(I), TBTA (tris(benzyltriazolylmethyl)amine), and ethyl vinyl

Table 1. Molecular Weight Data, Polydispersities, and Synthetic Conditions for Statistical Copolymers 1−5 and 10−19 and the Homopolymer 6

entry	*n* [u]	*m* [u]	$M_{n,th}$ [Da]	$M_{n,GPC}$ [Da]	PDI	polymer	monomer **7** [mg]	monomer **8** [mg]	catalyst **9** [mg]
1	70	30	35 800	25 800	1.1	**10**	140	78	5
2	40	60	38 700	29 500	1.1	**11**	70	136	4.4
3	10	90	41 600	28 400	1.1	**12**	16	190	4.1
4	3	97	42 300	29 000	1.1	**13**	4.8	200	4
5	1	99	42 500	27 100	1.1	**14**	1.6	200	3.9
6	70	30	33 300	33 600	1.2	**15**			
7	40	60	37 300	36 000	1.1	**16**			
8	10	90	41 300	35 400	1.1	**17**			
9	3	97	42 200	32 400	1.1	**18**			
10	1	99	42 500	29 300	1.1	**19**			
11	70	30	83 000	*a*	*a*	**1**			
12	40	60	65 700	47 200	1.3	**2**			
13	10	90	48 400	34 300	1.2	**3**			
14	3	97	44 400	33 200	1.2	**4**			
15	1	99	43 200	27 500	1.2	**5**			
16	0	100	42 600	33 300	1.1	**6**			

[a] Insoluble in THF, hardly soluble in DMF.

ether were purchased from Aldrich and used as received. The homopolymer (**6**) was prepared according to previous procedures.[14]

Synthesis of the Bromo-Functionalized Statistic Copolymers (10−14). In a dry beaded rim bottle which was thoroughly flushed with argon a solution of exo-*N*-(4,4,5,5,6,6,7,7,7-nonafluoroheptyl)-10-oxa-4-azatricyclodec-8-ene-3,5-dione (**8**) and exo-*N*-(6-bromohexyl)-10-oxa-4-azatricyclo-dec-8-ene-3,5-dione (**7**)[14] in dry and deoxygenated dichloromethane (10 mL) was prepared. A solution of benzylidene−bis(tricyclohexylphosphine)dichlororuthenium (**9**) in dichloromethane (1 mL) was added quickly to the reaction solution, which was stirred vigorously for 35−40 min. After complete monomer conversion (as monitored by TLC) the reaction mixture was quenched with ethyl vinyl ether, and the crude polymer was evaporated to dryness. Precipitating twice from dichloromethane in methanol yielded bromo-functionalized statistic copolymers (**10**−**14**) as light brown solids. Details on quantities of the reagents are given in Table 1. Yields are always between 80 and 90% after precipitation of the polymers.

^{1}H NMR (200 MHz, $CDCl_3$): δ (ppm) = 6.08 (bs, CH_2═CH_2, trans), 5.80 (bs, CH_2═CH_2, cis), 5.03 (bs, CH−O−CH, cis), 4.46 (bs, CH−O−CH, trans), 3.70−3.20 (m, CH−C═O, N−CH_2, CH_2−Br), 2.30−1.70 (m, alkyl), 1.65−1.20 (m, alkyl). ^{13}C NMR (50 MHz, $CDCl_3$): δ (ppm) = 175.7, 130.8, 122.0−107.0 (multiplets, J^1_{FC} = 98 Hz, J^2_{FC} = 22 Hz), 81.0, 53.4, 52.3, 38.7, 33.6, 32.5, 28.3 (triplet, J^2_{FC} = 22 Hz), 27.6, 27.5, 25.9, 18.9.

Synthesis of Azide-Functionalized Statistic Copolymers (15−19). Sodium azide was added to a solution of statistical copolymers (**10**−**14**) in DMF (10 mL), and the reaction was stirred for 6−8 h at room temperature. The solvent was completely removed under reduced pressure; the residue was resuspended in $CHCl_3$, filtrated through a syringe filter, concentrated, and evaporated to dryness, yielding azide functionalized statistic copolymers (**15**−**19**) as light brown solids. *Additional notes:* To obtain azide-functionalized statistic copolymers (**15**−**19**) with narrow molecular weight distribution, it is imperative to keep the reaction at ambient temperature and the reaction time as short as possible (6−8 h). Longer reaction times as well as higher temperature may lead to cross-linking via an intramolecular dipolar cycloaddition reaction. All azide-functionalized polymers have to be stored at (−20 °C). Detailed data for the individual polymers: polymer **15** (200 mg of polymer **10**; 55 mg of NaN_3; yield: 192 mg of polymer **15**); polymer **16** (190 mg of polymer **11**; 28 mg of NaN_3; yield: 175 mg of polymer **16**); polymer **17** (200 mg of polymer **12**; 5 mg of NaN_3; yield: 195 mg of polymer **17**); polymer **18** (180 mg of polymer **13**; 3 mg of NaN_3; yield: 173 mg of polymer **18**); polymer **19** (180 mg of polymer **14**; 1 mg of NaN_3; yield: 180 mg of polymer **19**).

^{1}H NMR (200 MHz, $CDCl_3$): δ (ppm) = 6.08 (bs, CH_2═CH_2, trans), 5.79 (bs, CH_2═CH_2, cis), 5.02 (bs, CH−O−CH, cis), 4.45 (bs, CH−O−CH, trans), 3.70−3.20 (m, CH−C═O, N−CH_2, CH_2−N_3), 2.30−1.75 (m, alkyl), 1.70−1.20 (m, alkyl). ^{13}C NMR (50 MHz, $CDCl_3$): δ (ppm) = 175.5, 130.8, 122.0−107.0 (multiplets, J^1_{FC} = 98 Hz, J^2_{FC} = 22 Hz), 82.2, 80.9, 53.3, 52.2, 51.1, 38.7, 28.6, 27.4, 26.2, 26.1, 18.9.

Synthesis of Statistic Copolymers That Exhibit Hamilton Receptor Functionalities (1−5). A solution of azide-functionalized statistic copolymers (**15**−**19**), 5-hex-5-ynoylamino-*N*,*N*′-bis(6-octanoylamino-pyridin-2-yl)isophthalamide (**20**),[2b] tetrakis(acetonitrile)hexafluorophosphate copper(I), TBTA (tris(benzyltriazolylmethyl)amine), and *N*,*N*-diisopropylethylamine in a solvent mixture of deoxygenated DMF (6 mL), toluene (1.5 mL), and water (0.1 mL) was stirred at ambient temperature for 48 h. The reaction mixture was evaporated to dryness and precipitated twice from THF or dichloromethane in methanol, yielding Hamilton receptor-functionalized statistic copolymers (**1**−**5**) as brown solids. Details for the individual polymers: polymer **1** (40 mg of polymer **15**; 120 mg of **20**, 4.5 mg of TBTA, 0.058 mL of DIPEA, 3.1 mg of tetrakis(acetonitrile) hexafluorophosphate copper(I); yield of polymer **1**: 72 mg); polymer **2** (60 mg of polymer **16**; 91 mg of **20**, 3.5 mg of TBTA, 0.044 mL of DIPEA, 2.4 mg of tetrakis(acetonitrile)-hexafluorophosphate copper(I); yield of polymer **2**: 78 mg); polymer **3** (80 mg of polymer **17**; 28 mg of **20**, 1 mg of TBTA, 0.013 mL of DIPEA, 0.3 mg of tetrakis(acetonitrile)hexafluorophosphate copper(I); yield of polymer **3**: 89 mg); polymer **4** (100 mg of polymer **18**; 10 mg of **20**, 0.4 mg of TBTA, 0.005 mL of DIPEA, 0.3 mg of tetrakis(acetonitrile)hexafluorophosphate copper(I); yield of polymer **4**: 97 mg); polymer **5** (100 mg of polymer **19**; 3.4 mg of **20**, 0.17 mg of TBTA, 0.002 mL of DIPEA, 0.09 mg of tetrakis-(acetonitrile) hexafluorophosphate copper(I); yield of polymer **5**: 93 mg).

Additional note: The "click" reaction should not be performed above ambient temperature due to an internal cycloaddition reaction. Because of the low solubility of statistic copolymers **1** and **2** in $CDCl_3$ and DMSO-d_6,^{13}C NMR spectra could not be obtained, especially at a concentration of few milligrams per milliliter. GPC measurements confirmed that 5-hex-5-ynoylamino-*N*,*N*′-bis(6-octanoylaminopyridin-2-yl)isophthalamide (**20**) was completely removed from polymers **1**−**5**.

^{1}H NMR (200 MHz, $CDCl_3$): δ (ppm) = 6.07 (s, 1.4H, trans), 5.81 (s, 0.6H, cis), 5.04 (s, 0.4H, cis), 4.44 (s, 1.6H, trans), 3.57 (bs, 2H), 3.34 (bs, 2H), 2.30−1.80 (m, 4H). ^{13}C NMR (50 MHz, $CDCl_3$): δ (ppm) = 175.4, 130.8, 122.0−107.0 (multiplets, J^1_{FC} = 98 Hz, J^2_{FC} = 22 Hz), 82.2, 80.8, 53.4, 52.2, 37.9, 28.6 (t, J^2_{FC} = 22 Hz), 19.0.

Synthesis of Exo-*N*-(4,4,5,5,6,6,7,7,7-nonafluoroheptyl)-10-oxa-4-azatricyclodec-8-ene-3,5-dione (8). A solution of 4,4,5,5,6,6,7,7,7-nonafluoro-heptan-1-ol (1.0 g, 3.60 mmol) and tetrabromomethane (1.878 g, 5.663 mmol) in dry CH_2Cl_2 (20 mL) was cooled to 0 °C, and a solution of triphenylphosphine (1.415 g, 5.393 mmol) in dry CH_2Cl_2 (5 mL) was added slowly. The ice bath was removed, and the mixture was stirred for 12 h at ambient temperature. After complete conversion the solvent was removed under reduced pressure, and the crude bromo compound was subsequently

Scheme 1. Synthesis of the Statistical Copolymers 1−5 Bearing the Supramolecular Receptor in a Variable Density within Their Chains

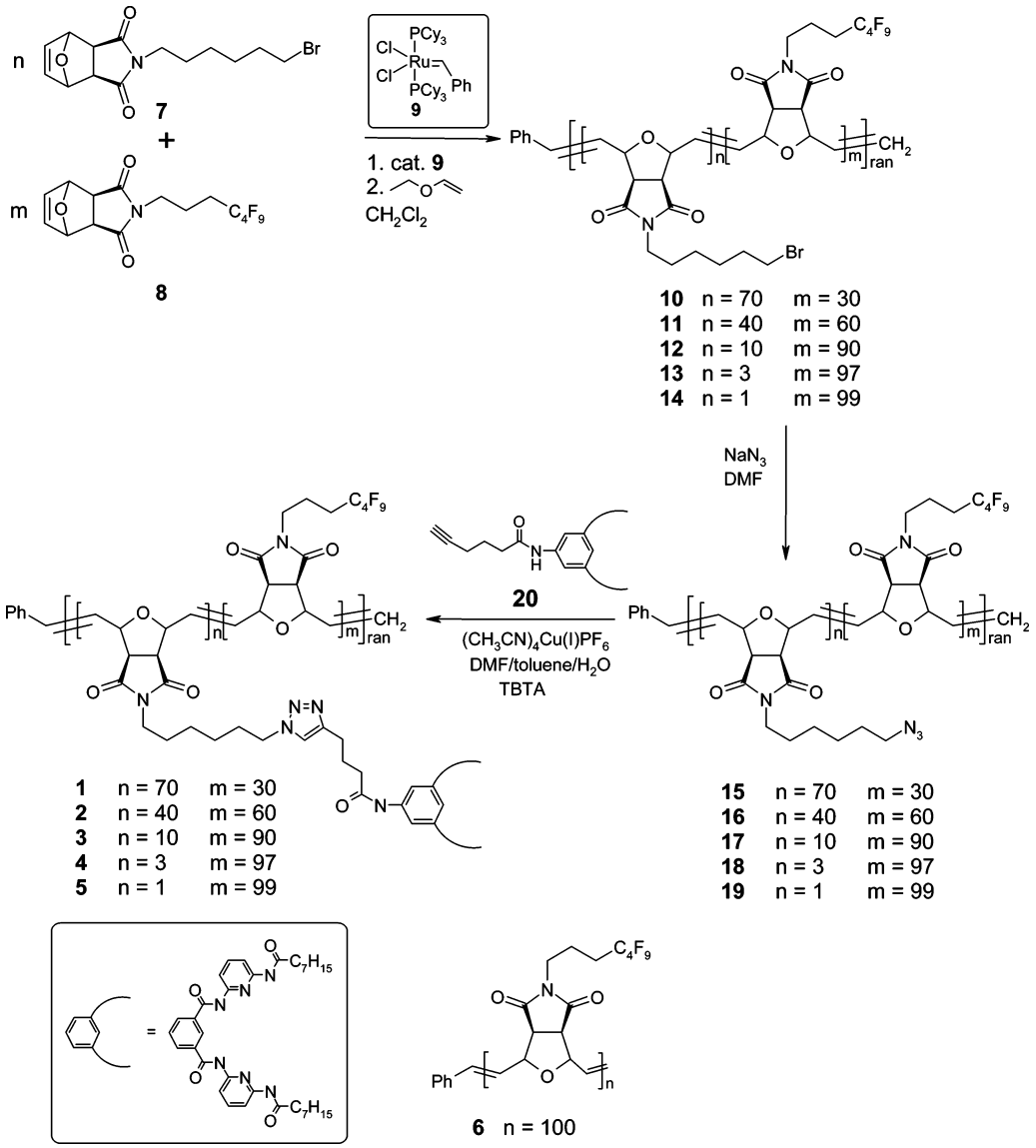

substituted without any further purification. Potassium carbonate (1.098 g, 7.910 mmol) and exo-10-oxa-4-azatricyclodec-8-ene-3,5-dione (0.653 g, 3.955 mmol) was added to crude 7-bromo-1,1,1,2,2,3,3,4,4-nonafluoroheptane and resuspended in dry DMF (60 mL). The reaction was stirred for 16 h at ambient temperature, and the solvent was removed subsequently under reduced pressure. Crude **8** was purified by chromatography (SiO_2, hexane/ethyl acetate = 2/1) in order to yield white crystals. Yield: 1.439 g (3.384 mmol, 94%); mp: 65−66 °C. ^{1}H NMR (200 MHz, $CDCl_3$): δ (ppm) = 6.48 (s, 2H), 5.23 (s, 2H), 3.54 (t, 2H), 2.83 (s, 2H), 2.01 (m, 2H), 1.85 (m, 2H). ^{13}C NMR (50 MHz, $CDCl_3$): δ (ppm) = 176.1, 136.4, 121.5−105.0 (multipletts, J^1_{FC} = 98 Hz, J^2_{FC} = 22 Hz), 80.9, 47.3, 37.7, 28.1 (t, J^2_{FC} = 23 Hz), 18.7.

Preparation of Smooth Polymer Films by Spin- and Dip-Coating. Silicon wafers were cut in squares of 8 × 8 mm using a glass cutter, cleaned from dust and silicon splinters with a stream of nitrogen, and incubated into a dust-free ethanol solution (filtrated through a syringe filter) for 5−10 min. From this solution they were quickly removed and immediately dried with a strong stream of nitrogen in order to prevent solvent margins obtained from evaporation. Subsequent UV irradiation for 15 min completely oxidized the surface and removed the last organic impurities on the wafers, which was again followed by cleaning with nitrogen. All wafers were stored in small and clean glass/plastic jars until they were used for coating. Polymer solutions were prepared directly before use. The amount of polymer was calculated for a 3−5 mL solution, setting the final concentration between 0.5 wt % (dip coating) and 1−2 wt % (for spin-coating). As soon as the polymer was completely solubilized, it was again applied through a syringe filter into a glass vessel (dip coating) or onto a silicon wafer (spin-coating). For film preparation via spin-coating techniques the silicon wafers were cleaned by a strong stream of nitrogen. Subsequently, they were placed on a spin-coater, and 1−2 drops of a completely dust-free polymer solution were applied onto the silicon wafer and the rotation disk was accelerated to the required rotation speed. After about 1 min the disk was decelerated. After cleaning the wafer again by a stream of nitrogen it was placed into a clean glass or plastic jar and stored under exclusion of light at 0 °C. To prepare polymer films via dip-coating techniques, the silicon wafers were cleaned by a strong stream of nitrogen and statically affixed and the dip-coating sequence was started. Once the dip-coating sequence is ended, the silicon wafers were cleaned by a stream of nitrogen, placed into a clean glass or plastic jar, and stored under exclusion of light at 0 °C.

Annealing of the Films. The prepared polymer films on the silicon wafers were cleaned with a strong stream of nitrogen and put into a 250 mL round-bottomed flask. The flask was evacuated to $\sim 10^{-3}$ bar and put into a preheated oil bath under protection from light. After complete annealing, the wafers were allowed to cool and the vacuum was removed. The silicon wafers were

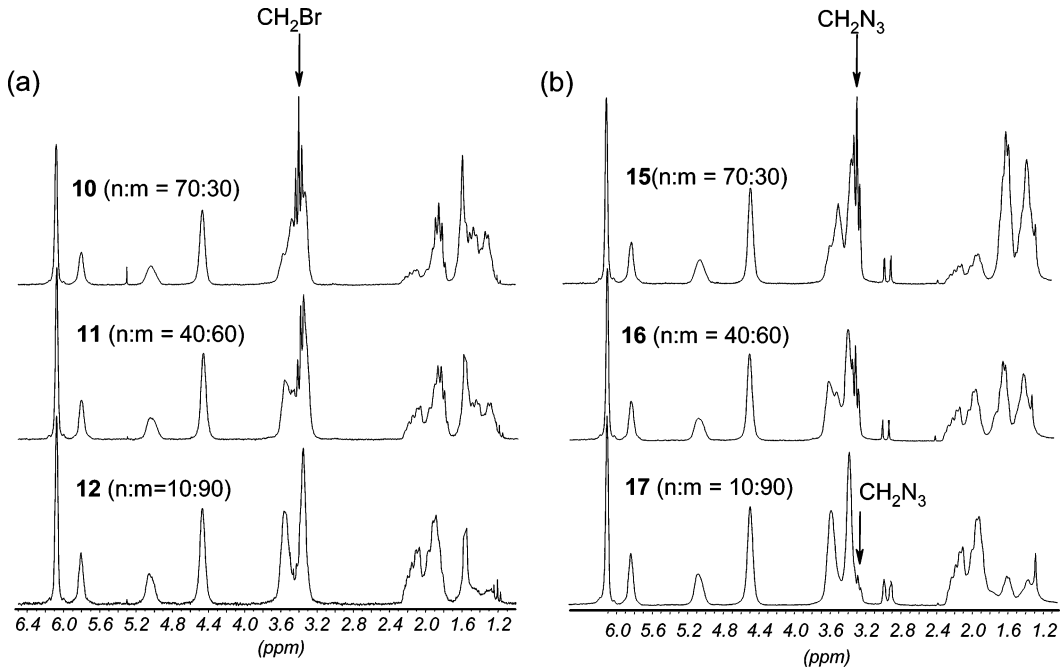

Figure 2. NMR spectra of (a) polymers **10**−**12** bearing the bromo substituents and (b) polymers **15**−**17** bearing the substituted azido moiety. The shift and transformations are readily seen and indicated by an arrow.

carefully withdrawn, cleaned with a strong stream of nitrogen and placed into a clean glass or plastic jar, and stored under exclusion of light at 0 °C.

Au nanoparticles (5 nm, bearing barbituric acid moieties or octadecyl moieties) were prepared according to the literature.[2b]

Nanoparticle Binding. Nanoparticle solutions of 0.1−0.3% in toluene were sonicated for 5 min prior to use and directly used for the assembly experiments onto the polymer films. Assembling nanoparticles onto polymeric films was carried out at room temperature in toluene solutions for 16 h without stirring. The films were purified by alternating washing steps in toluene and ethanol and subsequently blow-dried with nitrogen gas. Then, AFM experiments were performed directly on these substrates. In detail, a lower and a higher set point was made, and the resulting covered surface was evaluated using the photoshop program. The number of NPs per unit area was then determined manually by hand-counting of several smaller surface areas (500 nm × 500 nm) with subsequent statistical averaging.

Results and Discussion

Preparation of Statistical Copolymers. As mentioned in the Introduction, the generation of statistical copolymers bearing a defined density of supramolecular ligands in their chain was envisioned. As a starting point to our endeavor, we used the knowledge from block copolymers previously prepared by a combination of ROMP/click methodology[14] to prepare the present statistical copolymers **1**−**5** with a defined number of functional sites, ranging from 70 mol % of receptor to 1 mol % (see Scheme 1). Fluorinated side chains in monomer **8** were used in the comonomeric unit out of two reasons: (a) in order to effect an increased solubility and improved film formation in the subsequent polymeric copolymers after dip- and spin-coating and (b) due to the high structural similarity between monomer **8** and **7**, from which a highly statistical copolymerization can be expected. Starting from mixtures of the oxynorbornenes **7** and **8**, the copolymerization was initiated by use of the Grubbs catalyst **9**, subsequently quenching the reaction with ethyl vinyl ether. The overall number of monomeric units ($n + m$) in all final copolymers was calculated as 100. The monomer consumption was shown to be complete after 15 min as proven by ^{1}H NMR spectroscopy: no free monomer was observed in the mixture, furnishing copolymers **10**−**14** in high yields. Table 1 shows the data of molecular weights, with polydispersities ranging around $M_w/M_n = 1.1$ and molecular weights ranging from 25 900 to 29 000 g mol^{-1}. Subsequently, polymers **10**−**14** were transformed into the corresponding azides by reaction with sodium azide in dry *N*,*N*-dimethylformamide, leading to a quantitative formation of the corresponding azides **15**−**19** via nucleophilic substitution. The transformation was followed by ^{1}H NMR spectroscopy, as depicted in Figure 2. Thus, the conversion from the bromide-functionalized statistical copolymers **10**−**12** into the corresponding azides **15**−**17** is visible by a shift from 3.34 ppm (−CH_2Br) to 3.24 ppm (−CH_2N_3), indicating complete substitution of the bromide functionality. Copolymers with a smaller fraction of the comonomeric units (i.e., **13** and **14**) could not be monitored due to the low content of −CH_2Br unit within the copolymer. Now polymers **15**−**19** were subjected to the attachment of the supramolecular receptor unit **20**[2b] via the 1,3-dipolar cycloaddition "click" reaction. As demonstrated in previous examples,[2b,14,15] this reaction proceeds with excellent yields, furnishing a quantitative addition of the supramolecular unit onto the backbone of poly(oxynorbornene) polymers. The "click" reaction was therefore performed at ambient temperature in a ternary solvent mixture consisting of DMF/toluene/water in a ratio of 60/15/1. Tetrakis(acetonitrile)-hexafluorophosphate copper(I) as well as tris(1-benzyl-5-methyl-1*H*-[1,2,3]triazol-4-ylmethyl)amine (TBTA) were applied as catalytic systems furnishing the desired statistical block copolymers **1**−**5** quantitatively after 48 h. In a similar reaction pathway, the homopolymer **6** was prepared according to previous investigations.[14]

Generation of Polymer Films. Two different methods were investigated to generate polymer films of appropriate flatness and homogeneity: spin-coating and dip-coating. To evaluate principal issues of the film formation process, the statistical polymer **10** was used to optimize the parameters with regard to film thickness and film homogeneity. Thus, solutions of polymer **10** were spin-coated onto silicon wafers, and the resulting

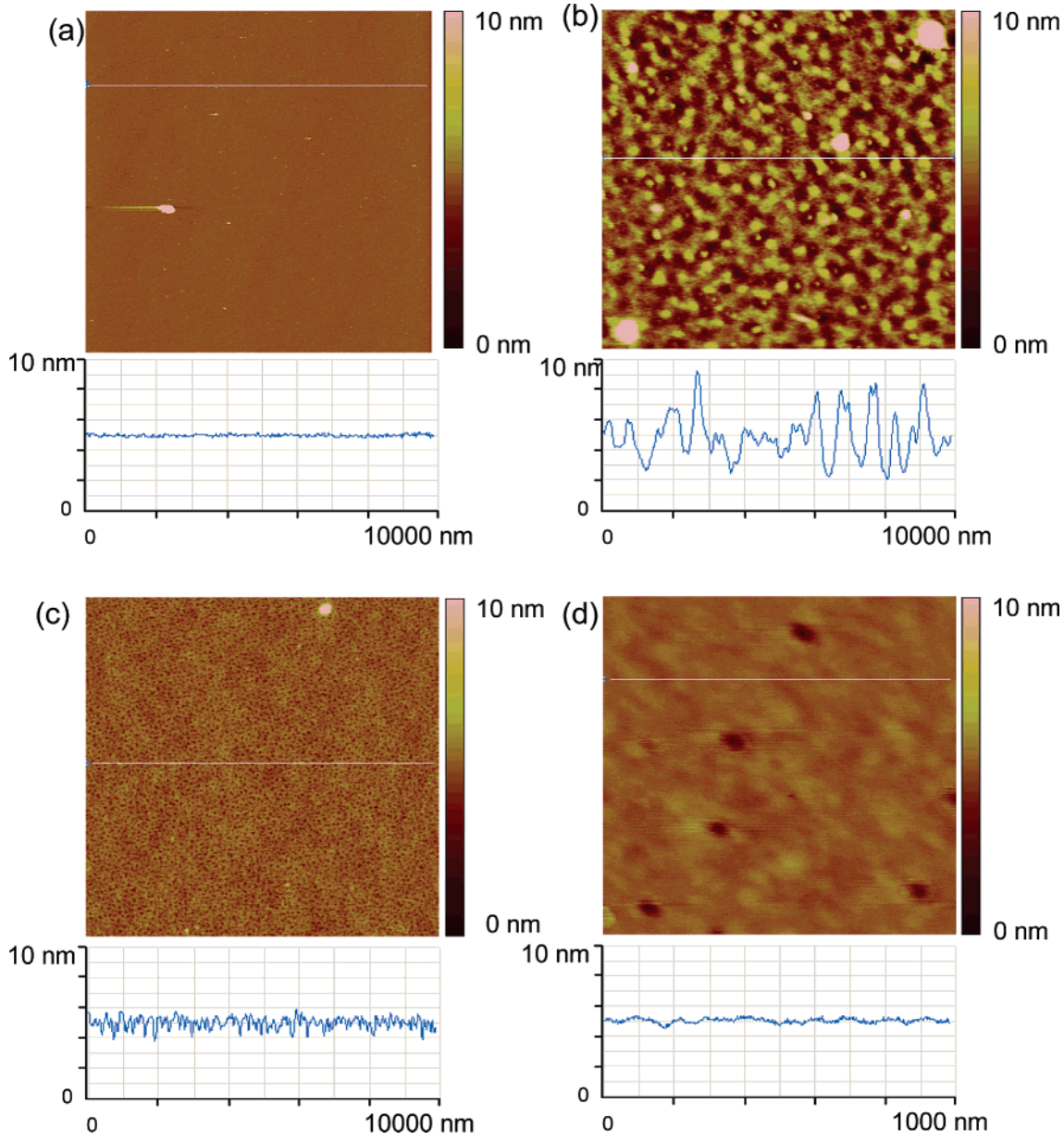

Figure 3. AFM images of polymer films obtained via spin-coating copolymer **10** from a chloroform solution onto a silicon wafer: (a) untreated silicon waver, $R_q = 0.08$ nm; (b) polymer film obtained from a 1 wt % solution at 2000 rpm, $R_q = 1.29$ nm; (c) polymer film obtained from a 1 wt % solution at 2600 rpm, $R_q = 0.39$ nm; (d) polymer film obtained from a 2 wt % solution at 2600 rpm, $R_q = 0.27$ nm.

surfaces were investigated toward different spin-coating parameters (i.e., solvent, spin rate, concentration, annealing) via AFM. The roughness data obtained were root-mean-square (rms $= R_q$) values, derived as standard deviation of all height values in an image. Figure 3 illustrates the results obtained by spin-coating polymer **10** from a chloroform solution by applying different spin rates and concentrations. Spin-coating polymer **10** from a 1 wt % solution at a spin rate of 2000 rpm resulted in a highly irregular polymer surface regarding its height profile (Figure 3b, $R_q = 1.29$ nm). To improve film smoothness, the spin rate was increased to 2600 rpm, reducing the root-mean-square value by a factor of 3 but also resulting in a polymer film that exhibited a high density of pore defects (1 nm depth) (Figure 3c, $R_q = 0.39$ nm). These holes could be removed by increasing the polymer concentration to 2 wt %, which finally lead to polymer films with a highly uniform surface profile (Figure 3d, $R_q = 0.27$). Although the resulting roughness values cannot compete with the ones obtained from an untreated atomic smooth silicon wafer (Figure 3a, $R_q = 0.08$ nm), they are by far sufficient in order to selectively detect nanoparticles of 5−7 nm in further binding studies.

Similar results were obtained when polymer **10** was spin-coated from a THF solution, although the trends toward surface−height profiles were found to be different. As illustrated in Figure 4, spin-coating from a 1.5 wt % solution at a spin rate of 2300 rpm resulted in an extremely inhomogeneous polymer film (Figure 4a, $R_q = 6.26$ nm). Because of an overly high substance load plateaus as well as valleys exerting an average height difference of up to 20 nm were formed (1−2 μm in diameter) that additionally exhibited microholes across the entire film. To reduce the substrate load, the spin rate was increased to 2900 rpm (Figure 4b, $R_q = 2.76$ nm) and the polymer concentration reduced to 1 wt % (Figure 4c, $R_q = 1.48$ nm), thus improving the average surface roughness by a factor of 4 but still not removing the 4 nm deep nanocavities. These holes were removed by annealing the preformed film at 70 °C for 48 h under vacuo, promoting equilibration of the surface profile (Figure 4d, $R_q = 0.30$ nm).

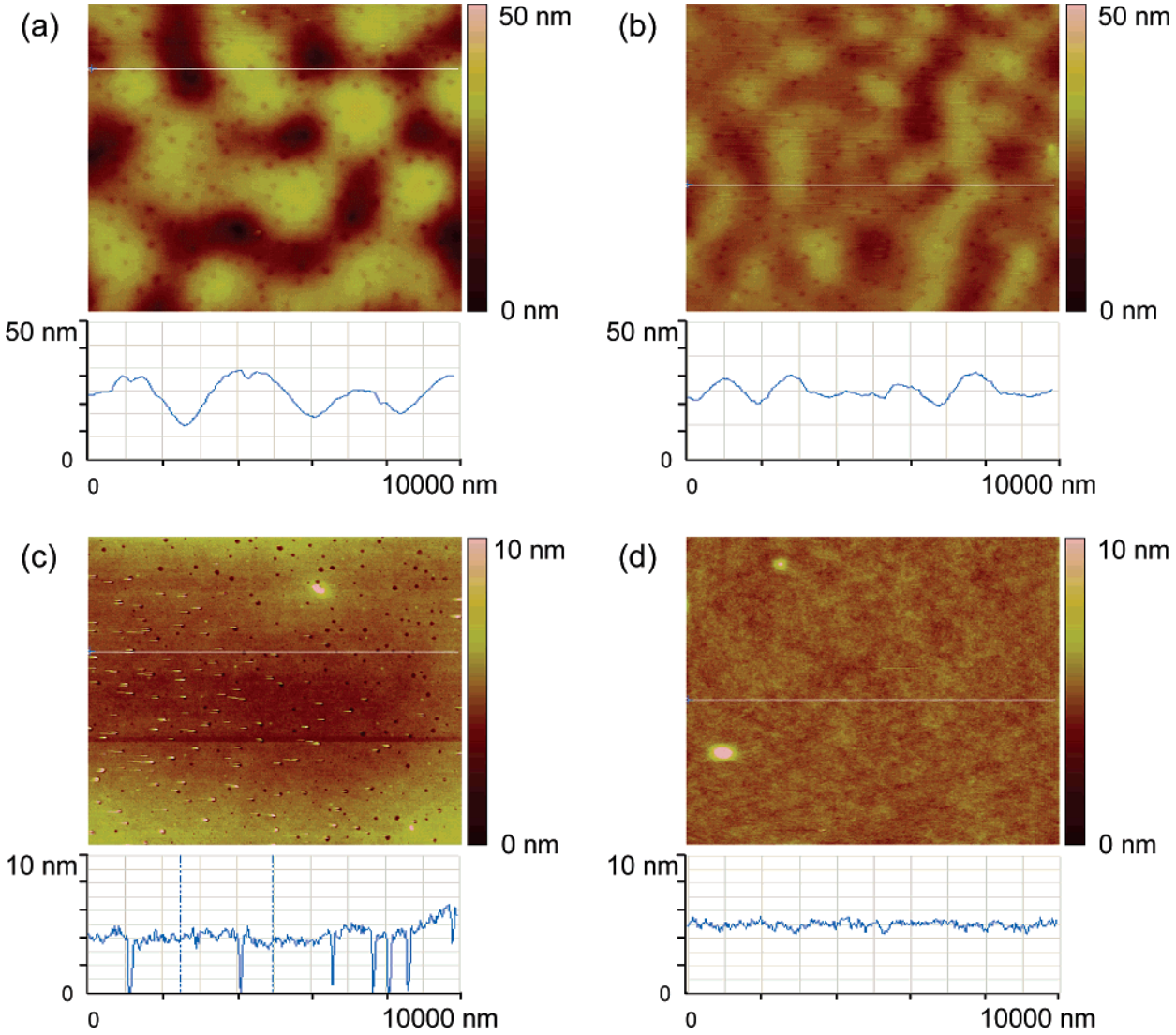

Figure 4. AFM images of polymer films obtained via spin-coating copolymer **10** from a THF solution onto a silicon wafer: (a) polymer film obtained from a 1.5 wt % solution at 2300 rpm, $R_q = 6.26$ nm; (b) polymer film obtained from a 1.5 wt % solution at 2900 rpm, $R_q = 2.76$ nm; (c) polymer film obtained from a 1 wt % solution at 2000 rpm, $R_q = 1.48$ nm; and (d) subsequent annealing at 70 °C for 48 h under vacuo, $R_q = 0.30$ nm.

Although similar results were obtained in the formation of smooth polymer films derived from polymer **10**, it became evident that finding the optimal spin-coating parameters was a tedious process. To simplify and generalize the formation of smooth polymer films, dip-coating techniques were explored thoroughly using polymer **5**, which displayed a good solubility in the solvents projected. Thus, a carefully pretreated silicon wafer (see Experimental Section) was dip-coated from a 0.5 wt % THF and chloroform solution of polymer **5** at a withdrawal speed of 3 mm/min. As illustrated in Figure 5, polymer films derived from both solvents exhibit a high density of pore defects although dip-casting from chloroform (Figure 5a) resulted in about doubled-sized microcavities (with respect to their circumference as well as depth) compared to surfaces obtained from THF (Figure 5b). Referring to the results obtained from spin-casting, thermal annealing at 80 °C for 48 h under vacuum resulted in the formation of highly uniform polymer surfaces ($R_q = 0.30$ nm) that lacked any type of microholes (Figure 5c). Thus, it was possible to develop a method in order to obtain highly uniform copolymer films that exhibited supramolecular domains distributed among the fluorinated parts of the statistical copolymer. Films of similar quality were prepared from polymer **3** ($n = 10$; $m = 90$: receptor density = 10 mol %) and polymer **4** ($n = 3$; $m = 97$: receptor density = 3 mol %). It was not possible to prepare films of appropriate quality starting from copolymers **1** and **2** displaying a high content of the supramolecular receptor, presumably due to their poor solubility both in THF and chloroform. Additionally, the spectrum of receptor densities was expanded by preparing surfaces with a receptor density of 0.1 and 0.01 mol %. Because of the fact that it was not possible to synthesize polymers with these monomer ratios, dip-coating solutions of polymer **5** (1 mol % receptor) were artificially diluted by a factor of 10 and 100 with the equally sized homopolymer **6** ($n = 100$), consisting entirely of the perfluorinated side chains. The films exhibited similar quality as those from the copolymers **3**−**5**. Thus, it was possible to generate polymer surfaces that exhibit only one Hamilton receptor for every 1000 (0.1 mol % receptor density) and 10 000 monomer units (0.01 mol % receptor density) (see Figure 5d,e). All prepared films therefore were ideally applicable for investigations toward supramolecular assembly of modified nanoparticles onto specific regions of polymer surfaces.

Binding Experiment with Nanoparticles. As experienced previously for block copolymeric films[6a] and self-assembled monolayers,[2b] binding experiments of the polymeric films with Au nanoparticles were conducted. Thus, all polymer surfaces

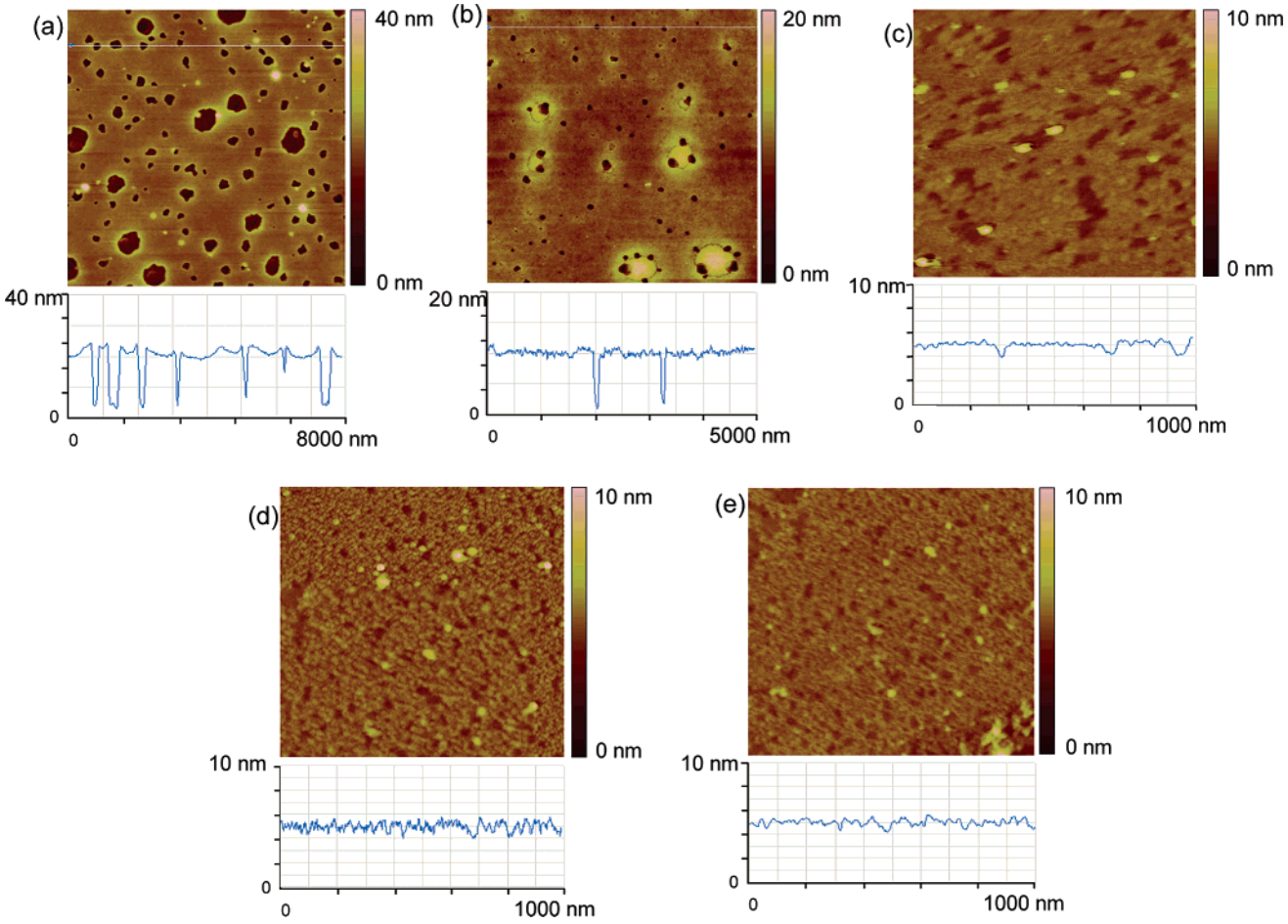

Figure 5. AFM images of polymer films obtained via dip-coating: (a) copolymer **5** dip-coated from a 0.5% chloroform solution; (b) copolymer **5** dip-coated from a 0.5% THF solution; (c) the film from experiment (b) after annealing for 48 h at 80 °C; (d) film obtained from a solution of copolymer **5** with homopolymer **6** (molar ratio: 1/10); (e) film obtained from a solution of copolymer **5** with homopolymer **6** (molar ratio: 1/100).

were incubated for 16 h with a toluene solution of barbituric acid-functionalized NPs (diameter = 5 nm). The resulting AFM images are illustrated in Figure 6 and Figure 7, displaying the deposited nanoparticles as height differences of ~5 nm. Reducing the receptor density from 10 mol % (Figure 6a) via 3 mol % (Figure 6b) toward 1 mol % (Figure 6c) led to only a moderate decrease of the bound nanoparticles on the polymeric films. The nanoparticle-covered area percentages of the respective surfaces were deduced by defining a threshold of 4 nm above the surface and subsequent graphical calculation of the covered surface. Thus, about 25 ± 5, 40 ± 5, and 25 ± 5 area % were found for the polymer films with 10, 3, and 1 mol % of supramolecular receptor present prior to the NP binding process. However, a significant decrease was observed when further reducing the receptor density up to a factor of 10 (Figure 7a) and 100 (Figure 7b). Thus, only very few nanoparticles are bound to surfaces displaying only 0.1 or 0.01 mol % of the matching receptor interaction, counting an area coverage of 15 ± 5% and 10 ± 5% of bound NP's. Therefore, a significant reduction of NP binding takes place at very low percentages of the supramolecular receptor present within the deposited statistical copolymer. Another important result is indicated upon the nonspecific binding of nanoparticles toward the polymeric films. As shown in Figure 7c, only random deposits were formed upon incubating a film derived from polymer **3** with Au nanoparticles (diameter = 5 nm) displaying an octadecyl ligand. Thus, in accordance with previous experiments on self-assembled monolayers (SAM's),[2b] nonspecific binding event occur only if no significant supramolecular receptor interaction is present.

Since the number of interactions present on the surface is an important factor, we have estimated the approximate number of supramolecular receptors on the respective polymeric surfaces, assuming that the area of one Hamilton receptor (dimension = 3.5 nm × 3 nm) is approximately $A_1 = 7$ nm^2, relating to a molecular volume of about $V_1 = 25$ nm^3.[2b] In a similar calculation, the molecular area of one monomeric unit (without the supramolecular receptor) counts to $A_2 = 3$ nm^2 and the molecular volume $V_2 = \sim 1$ nm^3 (based on the molecular dimensions of one oxynorbornene unit with a C_6 chain with $r = 0.45$ nm; height = 1,4 nm, calculated in a fully stretched conformation, assuming a cylindrical structure). Thus, the molecular volume of the attached receptor V_1 is larger by a factor of ~25 in comparison to the molecular volume of the monomeric unit V_2 within the polymer. On the basis of this rationale, a nearly dense layer of the supramolecular receptor is generated even when its molar fraction is only present at 1 mol % within the corresponding statistical copolymer in polymer **5**. With 5 nm Au NP's, about 3−4 barbituric acid moieties (on the NP's) can interact with the supramolecular receptor on the surface, leading to interaction energies (calculated from $\Delta G = -k_B T \ln(K_{assn})$, with $K_{assn} \sim 1 \times 10^5$ M^{-1}) of about $10k_BT$. Thus, at 1 mol % dilution, the polymer chains would cover about 100 nm^3 (100 units of monomeric units), with the supramolecular receptor (present in 1 mol %) occupying ~2.5 nm^3, leading to still ~1/50 of the overall volume covered with the supramolecular receptor. This accounts to an interaction energy of ~$1k_BT$ still in the thermal range and is thus sufficient for the NP binding onto such "diluted" surfaces.[9a,b] With further dilution, the

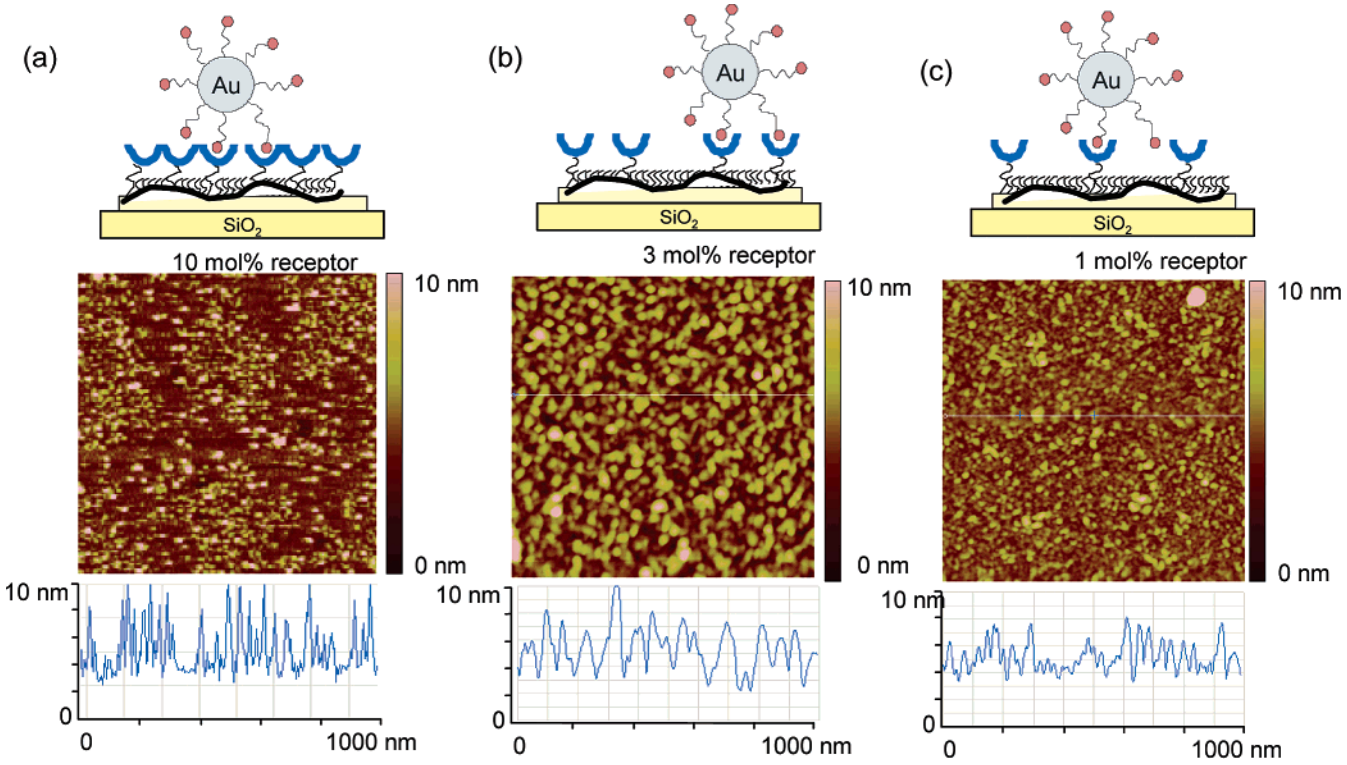

Figure 6. AFM images of barbituric NPs assembled onto surface exhibiting (a) 10 mol % (**3**), (b) 3 mol % (**4**), and (c) 1 mol % (**5**). Nanoparticles are visible as ~5 nm evelations above the film.

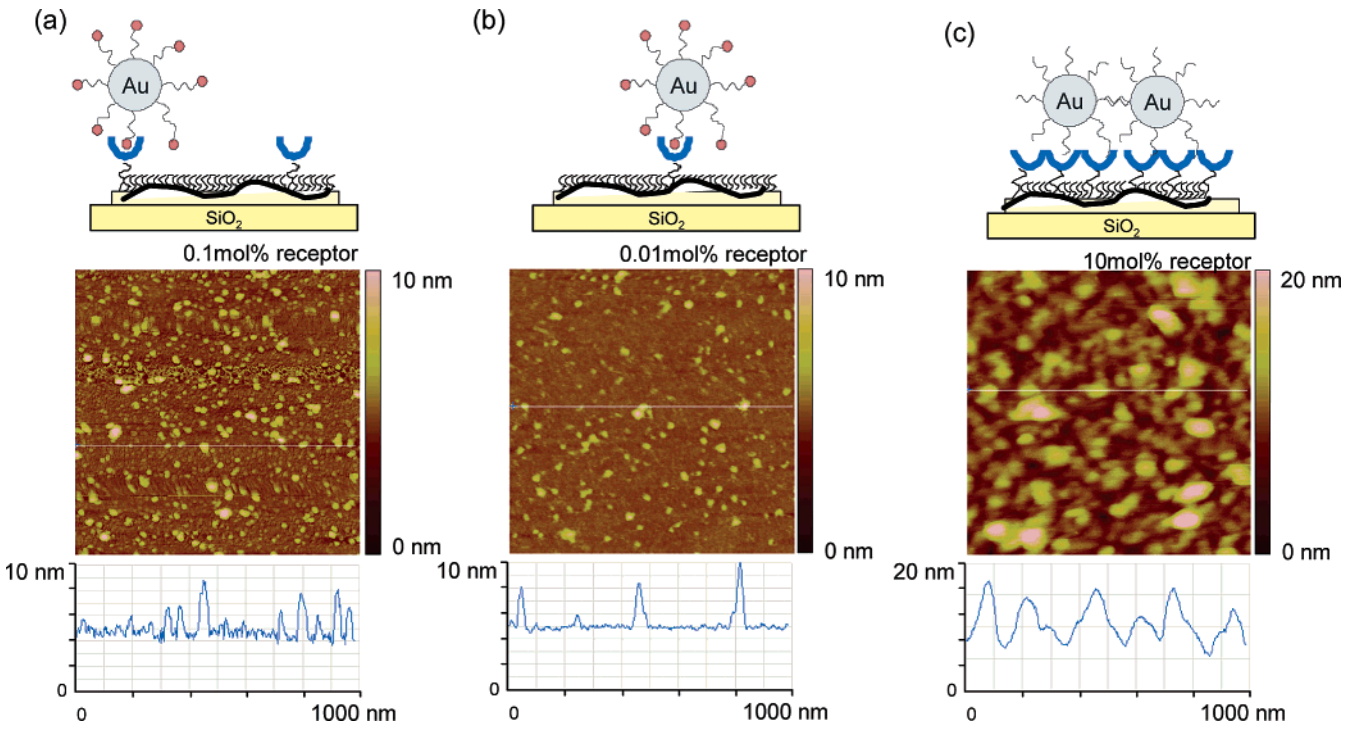

Figure 7. AFM images of barbituric acid-modified Au NPs assembled onto surface exhibiting (a) 0.1 and (b) 0.01 mol % of the supramolecular Hamilton receptor units. Nanoparticles are visible as ~5 nm evelations above the film. (c) AFM image of octadecyl-modified NPs nonselectively deposited onto the surface.

formation of diluted clusters is assumed, leading to the binding of still some nanoparticles to the surface, however, with lower density. Therefore, the number of nanoparticles bound to the surface does not change significantly upon investigating the polymer films derived from either polymer **3**, **4**, or **5**. Only at significantly lower concentrations of the supramolecular receptor (i.e., upon dilution with the homopolymer **6**, leading to receptor concentrations of 0.1 and 0.01 mol %) is a significant reduction of binding visible.

Conclusion

We have systematically investigated copolymeric surfaces, where a significant, strong supramolecular interaction is "thinned out" and subsequently used to study the binding of Au

nanoparticles with matching interaction onto these surfaces. The statistical copolymers, consisting of two different monomers, were prepared by ROMP and subsequent functionalization of terminal azido moieties via the Sharpless "click" reaction. This enabled the preparation of statistical copolymers with the supramolecular interaction ranging from 70 to 1 mol %. The copolymers were cast into films by dip-coating and spin-coating techniques, with dip-coating technique emerging as the superior method to obtain thin and smooth films after thermal annealing. Surfaces with supramolecular receptor densities ranging from 10 to 0.01 mol % were obtained, either via direct dip-coating of the copolymers or in mixture with a miscible homopolymer devoid of supramolecular interactions. Au nanoparticles were bound onto these surfaces, revealing a dependence on the supramolecular receptor densities only at 1% and below. The method therefore offers the generation of layers with a defined NP density, which easily can be estimated via geometric factors and interaction strengths. Moreover, the binding of a large variety of nanoparticles with different core structures can be envisioned.

Acknowledgment. We thank a grant from the Austrian Science Foundation FWF (project FWF 18740-B03) for financial support.

References and Notes

(1) (a) Haryono, A.; Binder, W. H. *Small* **2006**, *2*, 600−611 and references therein. (b) Glass, R.; Möller, M.; Spatz, J. P. *Nanotechnology* **2003**, *14*, 1153−1160. (c) Murray, C. B.; Kagan, C. R.; Bawendi, M. G. *Annu. Rev. Mater. Sci.* **2000**, *30*, 545−610.

(2) (a) Daniel, M.-C.; Astruc, D. *Chem. Rev.* **2004**, *104*, 293−346. (b) Zirbs, R.; Kienberger, F.; Hinterdorfer, P.; Binder, W. H. *Langmuir* **2005**, *21*, 8414−8421 and references therein. (c) Maury, P.; Peter, M.; Mahakingam, V.; Reinhoudt, D. N.; Huskens, J. *Adv. Funct. Mater.* **2005**, *15*, 451−457. (d) Mahaligam, V.; Onclin, S.; Peter, M.; Ravoo, B. J.; Huskens, J.; Reinhoudt, D. N. *Langmuir* **2004**, *20*, 11756−11762. (e) Crespo-Biel, O.; Dordi, B.; Reinhoudt, D. N.; Huskens, J. *J. Am. Chem. Soc.* **2005**, *127*, 7594−7600.

(3) Binder, W. H. *Angew. Chem., Int. Ed.* **2005**, *44*, 5172−5175 and references therein.

(4) Maenoso, S.; Okubo, T.; Yamaguchi, Y. *J. Nanoparticle Res.* **2003**, *5*, 5−15. (b) Bhat, R. R.; Genzer, J.; Chaney, B. N.; Sugg, H. W.; Liebmann-Vinson, A. *Nanotechnology* **2003**, *14*, 1145−1152.

(5) Hamley, I. W. *Nanotechnology* **2003**, *14*, R39−R54 and references therein.

(6) (a) Binder, W. H.; Kluger, C.; Straif, C. J.; Friedbacher, G. *Macromolecules* **2005**, *38*, 9405−9410. (b) Minelli, C.; Geissbuehler, I.; Eckert, R.; Vogel, H.; Heinzelmann, H.; Liley, M. *Colloid Polym. Sci.* **2004**, *282*, 1274−1278. (c) Minelli, C.; Hinderling, C.; Heinzelmann, H.; Pugin, R.; Liley, M. *Langmuir* **2005**, *21*, 7080−7082. (d) Zehner, R. W.; Sita, L. R. *Langmuir* **1999**, *15*, 6139−6141. (e) Zehner, R. W.; Lopes, W. A.; Morkved, T. L.; Jaeger, H.; Sita, L. R. *Langmuir* **1998**, *14*, 241−244.

(7) (a) Baron, R.; Huang, H.; Bassani, D. M.; Onopriyenko, A.; Zayats, M.; Willner, I. *Angew. Chem., Int. Ed.* **2005**, *44*, 4010−4015. (b) Pardo-Yissar, V.; Katz, E.; Wassermann, J.; Willner, I. *J. Am. Chem. Soc.* **2003**, *125*, 622−623.

(8) (a) Xu, H.; Hong, R.; Lu, T.; Uzun, O.; Rotello, V. M. *J. Am. Chem. Soc.* **2006**, *128*, 3162−3163. (b) Shenhar, R.; Jeoung, E.; Srivastava, S.; Norsten, T. B.; Rotello, V. M. *Adv. Mater.* **2005**, *17*, 2206−2210.

(9) (a) Lin, Y.; Böker, A.; He, J.; Sill, K.; Xiang, H.; Abetz, C.; Li, X.; Wang, J.; Emrick, T.; Long, S.; Wang, Q.; Balazs, A.; Russell, T. P. *Nature (London)* **2005**, *434*, 55−59. (b) Lin, Y.; Skaff, H.; Emrick, T.; Dinsmore, A. D.; Russell, T. P. *Science* **2003**, *299*, 226−229.

(10) (a) Huskens, J.; Deij, M. A.; Reinhoudt, D. N. *Angew. Chem., Int. Ed.* **2002**, *41*, 4467−4471. (b) Onclin, S.; Huskens, J.; Ravoo, B. J.; Reinhoudt, D. N. *Langmuir* **2004**, *20*, 13, 5460−5466. (c) Mulder, A.; Onclin, S.; Peter, M.; Hoogenboom, J. P.; Beijleveld, H.; ter Maar, J.; Garcia-Parajo, M. F.; Ravoo, B.; Huskens, J.; van Hulst, N. F.; Reinhoudt, D. N. *Small* **2005**, *1*, 242−253.

(11) (a) Credo, G. M.; Boal, A. K.; Das, K.; Galow, T. H.; Rotello, V. M.; Feldheim, D. L.; Gorman, C. B. *J. Am. Chem. Soc.* **2002**, *124*, 9036−9037. (b) Boal, A. K.; Frankamp, B. L.; Uzun, O.; Tuominen, M. T.; Rotello, V. M. *Chem. Mater.* **2004**, *16*, 3252−3256. (c) Carroll, J. B.; Frankamp, B. L.; Rotello, V. M. *Chem. Commun.* **2002**, 1892−1893. (d) Boal, A. K.; Ilhan, F.; DeRouchey, J. E.; Thurn-Albrecht, T.; Rotello, V. M. *Nature (London)* **2000**, *404*, 476. (e) Boal, A. K.; Rotello, V. M. *J. Am. Chem. Soc.* **1999**, *121*, 4917. (f) Boal, A. K.; Rotello, V. M. *Langmuir* **2000**, *16*, 9527−9532. (g) Chen, S.; Kimura, K. *Langmuir* **1999**, *15*, 1075−1082.

(12) (a) Binder, W. H.; Bernstorff, S.; Kluger, C.; Petraru, L.; Kunz, M. J. *Adv. Mater.* **2005**, 2824−2828. (b) Binder, W. H.; Kunz, M. J.; Kluger, C.; Hayn, G.; Saf, R. *Macromolecules* **2004**, *37*, 1749−1759. (c) Farnik, D.; Kluger, C.; Kunz, M. J.; Machl, D.; Petraru, L.; Binder, W. H. *Macromol. Symp.* **2004**, *217*, 247−266. (d) Binder, W. H. *Monatsh. Chem.* **2005**, 1−17. (e) Berl, V.; Schmutz, M.; Krische, M. J.; Khoury, R.; Lehn, J.-M. *Chem.—Eur. J.* **2002**, *8*, 1227−1244. (f) Tecilla, P.; Hamilton, A. D. *J. Chem. Soc., Chem. Commun.* **1990**, 1232−1234. (g) Chang, S.-K.; Hamilton, A. D. *J. Am. Chem. Soc.* **1988**, *110*, 1318−1319. (h) Chang, S.-K.; van Engen, D.; Hamilton, A. D. *J. Am. Chem. Soc.* **1991**, *113*, 7640−7645.

(13) Mammen, M.; Choi, S.-K.; Whitesides, G. M. *Angew. Chem., Int. Ed.* **1998**, *37*, 2754−2794.

(14) Binder, W. H.; Kluger, C. *Macromolecules* **2004**, *37*, 9321−9330.

(15) (a) Binder, W. H.; Kluger, C. *Curr. Org. Chem.* **2006**, *10*, 1791−1815. (b) Kolb, H. C.; Finn, M. G.; Sharpless, K. B. *Angew. Chem., Int. Ed.* **2001**, *40*, 2004−2021.

MA061256D